Atmos. Chem. Phys. Discuss., doi:10.5194/acp-2016-1166, 2017
Manuscript under review for journal Atmos. Chem. Phys.
Published: 7 February 2017
© Author(s) 2017. CC-BY 3.0 License.

Atmospheric Chemistry and Physics Discussions

Analyzing cloud base at local and regional scales to understand tropical montane cloud forest vulnerability to climate change

Ashley. E. Van Beusekom[1], Grizelle González[1], Martha A. Scholl[2]

[1]USDA Forest Service International Institute of Tropical Forestry, Jardín Botánico Sur, 1201 Calle Ceiba, Río Piedras, Puerto Rico 00926, United States
[2]US Geological Survey National Research Program, 12201 Sunrise Valley Drive, Reston, VA 20192, United States

Correspondence to: Ashley Van Beusekom (ashleyvanbeusekom@fs.fed.us)

Abstract. The degree to which cloud immersion provides water in addition to rainfall, suppresses transpiration, and sustains tropical montane cloud forests (TMCFs) during rainless periods is not well understood. Climate and land use changes represent a threat to these forests if cloud base altitude rises as a result of regional warming or deforestation. To establish a baseline for quantifying future changes in cloud base, we installed a ceilometer at 100 m altitude in the forest upwind of the TMCF occupying an altitude range from ~600 m to the peaks at 1100 m in the Luquillo Mountains of Eastern Puerto Rico. Airport ASOS ceilometer data, radiosonde data, and CALIPSO satellite data were obtained to calculate seasonal cloud base dynamics, altitude of the trade-wind inversion and typical cloud thickness for the surrounding Caribbean region. Cloud base is rarely quantified near mountains, so these results represent a first look at seasonal and diurnal cloud base dynamics for the TMCF. From May 2013 – August 2016, cloud base at Luquillo was lowest during the mid-summer dry season, and cloud bases were lower than the mountaintops as often in the winter dry season as in the wet seasons. The Luquillo low cloud base altitudes were higher than six other sites in the Caribbean by ~200-600 m, highlighting the importance of site selection to measure topographic influence on cloud height. Proximity to the oceanic cloud system where lower clouds are seasonally invariant in altitude and cover; along with orographic lifting and trade-wind generated cloud formation, may explain the dry season low clouds. The results indicate climate change threats to low-elevation TMCFs are not limited to the dry season; changes in synoptic-scale weather patterns that increase frequency of drought periods during the wet seasons (periods of higher cloud base) may also impact ecosystem health.

1 Introduction

Mountains play a key role in collecting atmospheric moisture in tropical regions (Wohl et al., 2012). Around 500 TMCFs have been identified world-wide on mountains with frequent cloud cover; these can be at higher elevation (on larger mountains) with lower temperatures, or lower elevation (on smaller mountains) with higher rainfall (Jarvis and Mulligan, 2011). The global set of TMCFs are almost all within 350 km of a coast and topographically exposed to higher-humidity air (Jarvis and Mulligan, 2011). Smaller mountains have lower temperatures and steeper adiabatic lapse rates from less solar radiation uptake (versus larger mountains, the mass-elevation effect), thus small mountains near the ocean can still support TMCFs despite having lower peak elevations (Foster, 2001; Jarvis and Mulligan, 2011).

Atmos. Chem. Phys. Discuss., doi:10.5194/acp-2016-1166, 2017
Manuscript under review for journal Atmos. Chem. Phys.
Published: 7 February 2017
© Author(s) 2017. CC-BY 3.0 License.

Atmospheric Chemistry and Physics Discussions

Up to 60% of the moisture input to TMCFs is derived from fog precipitation from low clouds (Bruijnzeel et al., 2011), but this value varies greatly from forest to forest. Cloud water has been deemed critical for the health of TMCFs, specifically for the abundant epiphytes which require consistent moisture input from the atmosphere (Gotsch et al., 2015). Fog adds moisture directly to the soil through the process of canopy interception and fog drip (Giambelluca et al., 2011), and indirectly alters the moisture budget through foliar uptake (Eller et al., 2013), lowering the saturation deficit of the atmosphere, and suppressing transpiration (Alvarado-Barrientos et al., 2014). For the low-elevation TMCF of this study, it might be expected that, given a relatively constant seasonal temperature lapse rate (within 0.1°C/1000 m for each season using previous study data (Van Beusekom et al., 2015)), wet seasons would have higher relative humidity caused by the larger amounts and spatial extent of rain events, and therefore lower clouds. Yet, previous field-based studies at four different low-elevation TMCFs found that similar or higher absolute amounts of fog precipitation were deposited during dry season measurements than during wet season measurements (Cavelier and Goldstein, 1989).

With their large energy inputs and fast rates of change spatially and temporally, tropical regions are some of the most dynamic atmospheric and hydrologic systems on Earth and thus may be significantly affected by climate change (Perez et al., 2016; Wohl et al., 2012). Regional cloud mass has been projected to decline with continued deforestation in maritime climates (van der Molen et al., 2006) and warming temperatures could raise cloud base in the global set of TMCFs (Foster, 2001; Still et al., 1999), which could lead to some low-elevation TMCFs losing cloud immersion. In the Caribbean, the wet seasons are projected to be less wet by the end of the century (Karmalkar et al., 2013). Specifically, 1) shallow convection over Caribbean mountains in the early rain season (ERS) may decrease if the trade-winds continue to strengthen and shift direction, changing sea breeze dynamics and weakening orographic lift (Comarazamy and González, 2011); and 2) the regional late rain season (LRS) may shorten due to strengthening of the Caribbean Low Level Jet (CLLJ) (Taylor et al., 2013). The Luquillo Mountains may have already undergone cloud base lifting since the first field studies in 1963; when cloud immersion was observed at 500 m (Odum and Pigeon, 1970) and at 600 m as noted in Weaver (1995).

The goal of this study was to determine cloud-base altitude and frequency of occurrence of low clouds during dry and wet seasons at a low-elevation TMCF in the Luquillo Mountains, Puerto Rico, to establish a baseline against which to quantify future change. In addition, ceilometer, radiosonde, and satellite data for the northern Caribbean were analyzed to determine how the surrounding region influences the cloud pattern. Ceilometer data that are available to the research community are usually collected at airports, not in mountainous areas, and furthermore do not specifically quantify cloud frequency (Schulz et al., 2016). A dedicated ceilometer was installed to measure cloud base altitudes on the windward side of the mountains, at 100 m elevation and 7 km distance from the ridgeline at ~1000 m, and metrics were developed to quantify seasonal changes in base altitude and frequency of low, mountain-associated clouds. These metrics can also be used in the future to analyze temporal trends.

Atmos. Chem. Phys. Discuss., doi:10.5194/acp-2016-1166, 2017
Manuscript under review for journal Atmos. Chem. Phys.
Published: 7 February 2017
© Author(s) 2017. CC-BY 3.0 License.

Atmospheric Chemistry and Physics Discussions

2 Study Area

The weather and clouds in the Luquillo Mountains follow patterns typical of the Caribbean region, which is dominated by the easterly trade-winds (Malkus, 1955; Odum and Pigeon, 1970; Taylor and Alfaro, 2005). The TMCF is located in the northern tropics at 18.3° N, 65.7° W. Annual trade-winds are driven by an interplay of the North Atlantic Subtropical High (NASH) sea level pressure system and the Inter-Tropical Convergence Zone (ITCZ) position (Giannini et al., 2000). In the northern hemisphere summer, the ITCZ moves to its northern position in the southwest Caribbean, weakening the trade-winds and giving way to the progression of tropical easterly low-pressure waves, which help to create a Caribbean wet season April/May through November (Gouirand et al., 2012). During winter the NASH extends westward, strengthening the trade-winds and suppressing convection to create a cooler dry season (DS) December through March (Gouirand et al., 2012). The CLLJ is a strengthening of the trade-winds in June and July, separating the rain season into early and late (ERS and LRS) with a warm drier season called the mid-summer drought (MSD) (Taylor et al., 2013). Trade-wind cumulus over the ocean are found within the trade-wind moist layer, limited above by the trade-wind inversion (TWI) and below by the lifting condensation level (LCL) (Stevens, 2005). Intra-annual variation in oceanic cloud cover is dampened as an estimated two-thirds of the cloud cover comes from annually-consistent clouds near the LCL; the other third is seasonally-changing clouds higher aloft (Nuijens et al., 2014). A pattern of lower clouds (bases and tops) over the ocean and higher clouds over the land with more diurnal effect of convection has been seen over the tropics with Cloud-Aerosol Lidar and Infrared Pathfinder Satellite Observation (CALIPSO) (Medeiros et al., 2010). However, with overpasses every 16 days, satellite data do not provide the level of temporal and spatial resolution to effectively study the clouds at a TMCF (Costa-Surós et al., 2013). Satellite data in this work are used to generalize the ceilometer findings and quantify patterns of cloud top height and cloud thickness in the region.

Experiments and long-term monitoring in the Luquillo mountains showed that orographic precipitation events occur consistently throughout the year (from the trade-winds and thermal lifting over the mountains), providing 25% of the rainfall by volume (Scholl and Murphy, 2014) as well as additional, unmeasured cloud water. Low clouds at the mountains have been hypothesized to originate with strong winds carrying oceanic clouds to the mountains too rapidly for dissipation (Raga et al., 2016), and additional condensation may occur with topographic forcing of moist air up the slopes. The cloud forest has been reported from near 600 m where epiphytes first occur in abundance and trees are noticeably smaller (Bruijnzeel et al., 2011; Weaver and Gould, 2013); in the Luquillo Mountains this elevation will vary with interactions between the topography and wind direction (e.g. the TMCF elevation range is almost certainly higher on the leeward slopes). Peak elevation is 1077 m. Seasonal patterns of clouds in the Luquillo TMCF were studied with synoptic weather observations (Malkus, 1955; Odum and Pigeon, 1970) and more recently there have been summer cloud water deposition measurements (Eugster et al., 2006; Holwerda et al., 2011).

Atmos. Chem. Phys. Discuss., doi:10.5194/acp-2016-1166, 2017
Manuscript under review for journal Atmos. Chem. Phys.
Published: 7 February 2017
© Author(s) 2017. CC-BY 3.0 License.

Atmospheric Chemistry and Physics Discussions

3 Methods

A Vaisala CL31 laser ceilometer was installed at 100 m elevation 7 km northeast of the ridge line collected data at 30-second intervals April 29, 2013 through August 1, 2016. Raw ceilometer data used in this study were the altitudes of the lowest cloud layer at a point above the instrument, determined by a visibility defined according to a 5% contrast threshold, and the bottom of 100 m of no vertical visibility defined as the cloud base (http://www.vaisala.com). The mean and median cloud base values that are usually calculated from ceilometer data are not sufficient to answer our questions about the frequency of clouds immersing the relatively low-elevation forested mountains, because raw data from a point source include numerous clear-sky and high cloud base observations. Therefore we developed metrics to summarize the cloud base altitude data in ways that could express differences and changes (temporally and spatially) in cloud base for altitude ranges of interest in the TMCF, which occupies elevations from ~600-1077 m at this site (Weaver and Gould, 2013). The metrics were derived from the frequency distributions of all cloud base measurements, where clear-sky was considered an infinite cloud altitude in the computations and clouds that may have been present below the elevation of the ceilometer (100 m) were not recorded. We did not trim the data to the altitude of interest; using all data gave a more complete picture of the climate of the entire atmosphere above the site. 'Hourly low cloud base' was defined as the altitude marking the first quartile (Q_1) of the 120 measurements in each hour, 'Daily low cloud base' was defined at the daily first tertile (T_1) of the distribution of Q_1 altitudes for each hour, meaning the low cloud base metric was at or below that altitude for 8 (not necessarily consecutive) hours in the 24-hour day. Hourly minimum cloud base was defined as the single-value altitude of the lowest cloud base detected during each hour. 'Daily minimum cloud base' was defined as the daily seventh octile (O_7) of the distribution of minimum values for each hour, meaning the minimum cloud base was at or below that altitude for 21 hours in the day. The daily low metric represents a cloud base altitude that is achieved often in the portion of the day with the lowest clouds; whereas the daily minimum metric represents an altitude that lowest cloud base is found at throughout most of the day. For comparison with regional Automated Surface Observation System (ASOS) data, the standard hourly average cloud bases and average cloud bases (omitting clear-sky data points) were also calculated at our site (Luquillo). Hourly cloud cover was computed as the fraction of positive cloud base detections, at any altitude, that occurred in the 120 measurements per hour of the raw data. Hourly rainfall, relative humidity (RH), temperature, wind speed, and wind direction data were collected at several weather stations around the TMCF within an 8 km^2 area for differing periods of record (PORs) (Table 1). High correlations were observed between these parameters across the stations for periods of overlap, giving confidence that weather immediately around the TMCF was homogeneous in pattern, though clearly not magnitude (Van Beusekom et al., 2015). Mean sea level pressure (MSLP) near the TMCF was highly correlated with the MSLP at the ASOS station TJNR, Ceiba (correlation coefficient $\rho = 0.98$). The rainfall and RH data at 361 m and the MSLP at 100 m (missing values filled with data from Ceiba) were representative of seasonal patterns in Luquillo and were used to correlate with the ceilometer data.

The 2000-2016 MSLP showed higher pressure in the dry seasons and lower pressure in the wet seasons (Fig. 1c), exemplifying the regional seasonal patterns that originate with the NASH and CLLJ (Brueck et al., 2014; Taylor et al., 2013). However, interannual variability in the timing of seasons from climate oscillations was observed in averages made

Atmos. Chem. Phys. Discuss., doi:10.5194/acp-2016-1166, 2017
Manuscript under review for journal Atmos. Chem. Phys.
Published: 7 February 2017
© Author(s) 2017. CC-BY 3.0 License.

Atmospheric Chemistry and Physics Discussions

over the shorter record (Gouirand et al., 2012). Rainfall, RH, and MSLP months April 1-15 (M4.5), October (M10), and December (M12) in the Luquillo ceilometer period of record (LQ POR, May 2013 through August 2016) were not representative of the longer period 2000-2016 (Fig. 1), and thus we omitted these time periods for each year in presentation of seasonal results for the ceilometer data.

The ASOS data for six airport stations in the Northern Caribbean from 2000-2016 were accessed from the Iowa Environmental Mesonet (Fig. 4a, Table 1), which include average hourly cloud base when clouds exist, cloud cover as percentage of the sky, and observed weather variables. No 30-second data were available and all data have been summarized to the mean-hour before reporting, thus not specifically quantifying cloud frequency. The ASOS network reports by a range of oktas covered by cloud (Nadolski, 1998): "clear" for 0, "few" for 1/8-2/8, "scattered" for 3/8-4/8, "broken" for 5/8-7/8, and "overcast" for 8/8. These numbers are automatically calculated by the instrument from 30-second detections similar to our calculations at Luquillo (Nadolski, 1998). For calculation of average POR cloud cover in this study, the cover categories were converted to sky cover fraction using the middle of the range or 0 for "clear", 0.125 for "few", 0.375 for "scattered", 0.75 for "broken", and 1 for "overcast".

To characterize variations in the cloud-system of the entire region, metrics were developed to summarize the hourly average cloud base data at the ASOS stations and Luquillo in ways that expressed the changes in seasonal altitudes of clouds at altitudes meaningful for heights in the TMCF. 'Daily minimum mean-hour cloud base' was defined as the minimum value of the hourly averages each day and similarly 'daily maximum mean-hour cloud base' was defined as the value of the maximum mean-hour. 'Daily low mean-hour cloud base' was defined as the daily Q_1 of the hourly averages. To characterize the cloud-system at large, mean hourly cloud cover (in fraction of sky) was also calculated.

In order to represent usual atmospheric conditions, bearing in mind the data were mean-hours of existing cloud bases and not representing clear conditions that may have been present during the hour, hourly average cloud base was considered clear sky (in calculation of the daily metrics) if the cloud cover fraction was less than 50% of a station's POR mean cloud cover. POR mean cloud cover was 0.6 fraction of the sky at Luquillo (foothills) but 0.2-0.3 fraction of the sky at the ASOS stations (airports). Under this condition, ~2% of the data at each station were removed before calculation of 'usual' conditions.

Two to three times daily, radiosonde profiles were available for 2000-2016 at Santo Domingo, San Juan, and Sint Maarten from the Integrated Global Radiosonde Archive (Durre et al., 2009). We expected to find cloud base altitudes above the LCL and cloud tops at or below the TWI for trade-wind conditions (Brueck et al., 2014; Malkus, 1955), thus we used the radiosonde profiles to compute values of minimum LCL and maximum TWI base over each day to quantify frequency of stable marine boundary layers and trade-wind cloud conditions at the site (Rastogi et al., 2016). The LCL calculation used the method of Bolton (1980) (for details see Appendix A). The TWI calculation used the method of Cao et al. (2007) with the published pressure bounds for the Atlantic (Augstein et al., 1974; for details see Appendix A).

CALIPSO satellite vertical feature mask data (Hunt et al., 2009) were analyzed for information on cloud tops and cloud thickness in the region. There are ten tracks in the region considered (Fig. 4a, Table 1); the northwest/southeast trending tracks are on the daytime orbit, and the other direction the nighttime orbit. Each track has 16 days until a repeat measurement

Atmos. Chem. Phys. Discuss., doi:10.5194/acp-2016-1166, 2017
Manuscript under review for journal Atmos. Chem. Phys.
Published: 7 February 2017
© Author(s) 2017. CC-BY 3.0 License.

Atmospheric Chemistry and Physics Discussions

and records if cloud was detected in 300 m horizontal by 30 m vertical cells up to 8.2 km altitude (data extend up to 30 km but we do not discuss those here). Data were summarized by fraction of measurements with cloud detections in larger cells of 0.05° latitude (approximately 6 km) by 30 m vertical.

All correlations between variables were computed as Pearson product-moment correlations with coefficient ρ measuring linear correlation. Strengths of correlations were based on the relationships between weather parameters and clouds found in this study and another Caribbean cloud and weather study (Brueck et al., 2014); correlation was assumed fair if $0.3 < |\rho| < 0.4$, good if $0.4 < |\rho| < 0.6$, and very good if $|\rho| > 0.6$. The regional means and correlations were also computed over the shorter LQ POR with exclusion of the non-representative months. These were not substantially different than the 2000-2016 results presented here (in Fig. 4, and Fig. 5, Table 3), but the mathematical strength of the resulting means and significance of the correlations necessarily decreased with less data.

4 Results

The data suggest that the TMCF has a greater probability of cloud interaction during the mid-summer dry season (MSD) throughout the entirety of the forest (between 600-1000 m), and during the winter dry season (DS) at the upper elevational reaches (<1000 m), than it does in the wet seasons (Figs 2, 3a). Of all the seasons, the MSD (Fig. 2c) had low and minimum cloud bases at 600-750 m most consistently. The cloud base levels in the DS (Fig. 2a) were not below 750 m as often as in the wet seasons, but were also absent above 3000 m, so on an hourly and daily basis, the low and minimum cloud bases were below 1000 m more consistently in the dry than in the wet seasons (summing the bars in Fig. 2). During the daytime hours (09:00-18:00) the median hourly low and minimum cloud bases were as low or lower in altitude in the dry seasons as the wet seasons (Fig. 3a); this was also the time of day when rainfall was the least frequent in the dry seasons (Fig. 3b). The means of median-hourly low and minimum cloud bases over the entire POR (the data shown in Fig. 3a) were 915 m and 702 m, respectively.

Of all available weather variables, the daily low and minimum cloud bases correlated best with RH and MSLP (negative correlations, Table 2, Figs 1a, c). Interestingly, RH did not correlate well with rainfall (Table 2) or with pressure indicators of wet and dry seasons (visually confirmed in Fig. 1b).

Over the North Caribbean region excluding Luquillo, the maximum cloud base altitudes were below the TWI and the lowest near the average LCL (both calculated from 2000-2016 radiosonde profiles, Fig. 4b). The TWI was distinguishable 86% of the time in the DS, 74% in the MSD, 71% in the ERS, and 65% in the LRS. The average TWI values were 1921 m for Santo Domingo, 2141 m for San Juan, and 1851 m for Sint Maarten, with average seasonal standard deviation of ±48 m and the lowest TWI altitudes in the MSD. This agrees with other research on global distribution and seasonal variance (Guo et al., 2011), and the influence of local topography (Carrillo et al., 2015). The average LCL values were 511 m for Santo Domingo and 607 m for San Juan, with average seasonal standard deviation of ±29 m and the lowest values in the ERS. For these stations, the LCL was distinguishable ~85% of the time in all seasons. At Sint Maarten, the POR-ceilometer-observed mean daily minimum cloud base was 272 m lower than the calculated mean LCL of 775 m (and the LCL was only distinguishable

Atmos. Chem. Phys. Discuss., doi:10.5194/acp-2016-1166, 2017
Manuscript under review for journal Atmos. Chem. Phys.
Published: 7 February 2017
© Author(s) 2017. CC-BY 3.0 License.

Atmospheric Chemistry and Physics Discussions

59% of the time), whereas at Santo Domingo and San Juan the difference was 10 m and 16 m lower, respectively. Consequently, we assumed the radiosonde measurements were not representative of conditions above the ceilometer location at Sint Maarten, and these data were not used in the regional comparison.

Regionally, the low cloud base from the mean-hours was lower during the MSD than during the other seasons at all of the stations, indicating seasonal variation in mean low cloud base altitude (Fig. 4c). However, the longer winter dry season, DS, had a higher low cloud base than the wet seasons except at Luquillo (note that at Luquillo in Fig. 4b, less frequent DS high clouds (see Fig. 1) lowers the mean-hour cloud base). Cloud cover percentage was highest in the MSD relative to the other seasons at all the stations to the east (windward) and including Luquillo, and DS cloud cover was similar to or higher than the wet seasons (Fig. 4d). The low and minimum cloud bases for stations near to Luquillo correlated much better with cloud cover than at the stations as a whole, with very good negative correlation at Luquillo itself (Table 2, S3).

In contrast to Luquillo (Fig. 1b) the regional pattern of RH for 2000-2016 was as expected, with lower RH during the dry seasons than the wet seasons (Fig. 5) and the low and minimum cloud bases all had fair correlation with the RH measurements (Table 3). Regionally, no metrics of daily clouds correlated with MSLP except at Luquillo, where the low and maximum cloud bases had good and very good correlation with MSLP, respectively (Table 3).

CALIPSO data showed that regionally, oceanic clouds were most likely to be found in a layer from 400 m to 1 km, and land with high topography increased the likelihood of clouds in a layer from land surface elevation up to 2 km, approximately the altitude of the TWI which under most conditions caps the trade-wind cumuli (Fig. 6). For the lowest cloud layer below 8.2 km on all ten tracks, only considering when clouds are present, the mean altitude of the base of the layer was 845 m over ocean and 934 m over land, and the mean altitude of the top of the layer was 1557 m over ocean and 1784 m over land: showing increase in cloud layer altitude over land. However, considering no layer to have infinite cloud base and top altitude, the Q_1 altitude of the base of the layer was 415 m over ocean and 265 m over land, and the Q_1 altitude of the top was 1045 m over ocean and 1225 m over land: showing that it was cloudier over land and there were more low-altitude cloud observations with the more cloud observations. Highest topography land (Fig. 6c) exhibited a limiting of the cloud layer around 2 km, however lower topography land had thicker clouds than over ocean. The mean layer thickness was 358 m over ocean and 531 m over land, as most land in the tracks was low topography.

5 Discussion and Conclusions

Caribbean trade-wind cumulus clouds have been observed by other studies as mostly being shallow and originating with bases near the LCL (Malkus, 1955; Nuijens et al., 2014; Zhang et al., 2012); our ceilometer data support this finding, with most oceanic cloud bases at or within 100 m the LCL (Figs 4 and 6). Both 5-day and monthly correlations between low clouds and RH were observed region-wide (Table 3). It has been theorized that a stronger TWI increases oceanic cloud cover and lowers the cloud base, and cloud amounts reflect the upstream conditions (Myers and Norris, 2013; Stevens, 2005). The Luquillo Mountains are ~10 km from the coast, and trade-wind velocity in the region is typically 3-5 m/s (Lawton et al., 2001). Existing clouds are over land for about 30 minutes before reaching the TMCF, and orographic lifting may generate

Atmos. Chem. Phys. Discuss., doi:10.5194/acp-2016-1166, 2017
Manuscript under review for journal Atmos. Chem. Phys.
Published: 7 February 2017
© Author(s) 2017. CC-BY 3.0 License.

Atmospheric Chemistry and Physics Discussions

additional condensation during parts of the daily cycle. We postulate that proximity of the TMCF to the coast is an ecological advantage in that the forest has adapted to the oceanic atmosphere (relatively invariant humidity, temperature profile, and cloud cover). The Caribbean ASOS stations windward of Luquillo may be influenced by the stable marine boundary layer TWI reflecting conditions closer to those over the ocean surface than to those on land. These stations have higher cloud cover in the dry seasons (Fig 3d) and lower clouds correlating with increasing cloud cover (Table 3); remnants of this weather pattern may be carrying on to land at Luquillo (Raga et al., 2016).

However, our results clearly show the changes that occur when the clouds interact with land that extends above the LCL in a trade-wind regime: cloud base altitude and cloud cover increased over the mountains compared to that over small low-relief islands or open ocean (Figs 4 and 6) and the cloud base rises high enough that a TWI limit to vertical extent of the clouds may result in shallower (thinner) cloud layers at the highest land elevations and cloud bases meeting the land (Fig. 6). When high-relief topography is close to the ocean this effect is especially pronounced, as seen on the northernmost peninsula of the Dominican Republic in the CALIPSO data (Fig 6a, b) and at the Luquillo ceilometer. The ceilometer data showed that the correlation of daily low and minimum cloud base metrics with RH was the result of including cloud bases lower than 1000 m in the calculations, and correlation of these metrics with MSLP was driven by including cloud bases greater than 1500 m in the calculations (Table 2). In addition, the relatively high RH during the dry seasons in the mountains is a pattern that is not seen over the low-relief sites (Figs 1b, 5) highlighting the importance of site-specific cloud base measurements for TMCFs, rather than relying on data from regional stations at airports.

Low-elevation TMCFs are especially vulnerable in a changing climate, because slight increases in cloud base altitude could end cloud immersion for the entire forest (Foster, 2001; Lawton et al., 2001; Ray et al., 2006). With these results, we question the likelihood of frequent cloud base at 600 m at Luquillo (Figs 2, 3), the published TMCF lowest elevation based on observed characteristic cloud forest vegetation of smaller trees (Weaver and Gould, 2013). It is possible that such vegetation may persist for some time after changing climatic conditions have lifted the cloud base (Oliveira et al., 2014). Rainfall and relative humidity in the forest are currently quite high, indicating that some species, once established, may be able to survive if rainfall remains high (Martin et al., 2011), but the diversity and numbers of epiphytes and other species that depend on cloud immersion will decline. In addition, the absence of water input from cloud deposition on the vegetation would change the precipitation/ evapotranspiration dynamics of the watersheds in the mountains to an unknown extent.

This study presented evidence that consistently as low, or lower, clouds exist in the dry seasons than in the wet seasons at a low-elevation TMCF under the current climate regime, indicating that the TMCF ecosystem may be more vulnerable to wet-season drought periods than was previously assumed. The Caribbean region is projected to undergo drying in the future, with various mechanisms that will suppress deep convection and frequent high rainfall (Karmalkar et al., 2013). If trade-wind clouds were thinner and shallow convection was weak during those periods, drought effects on the TMCF could be significant. Continued long-term measurements at Luquillo, and comparisons to other low-elevation TMCFs, are needed to expand the low cloud pattern temporally and geographically with full confidence, and to determine how projected changes in regional temperature and atmospheric circulation patterns will affect these cloud-water-dependent ecosystems.

Atmos. Chem. Phys. Discuss., doi:10.5194/acp-2016-1166, 2017
Manuscript under review for journal Atmos. Chem. Phys.
Published: 7 February 2017
© Author(s) 2017. CC-BY 3.0 License.

Atmospheric Chemistry and Physics Discussions

6 Data Availability

The Luquillo ceilometer data is hosted on Science Base https://www.sciencebase.gov and the Critical Zone Observatory Data Portal http://criticalzone.org/luquillo/data.

Appendix A

This Appendix includes further text detail on the calculation of the lifting condensation level (LCL) and the trade-wind inversion (TWI).

The LCL is the altitude at which a parcel of air cools to the temperature that its relative humidity is 100%. Assuming the presence of cloud condensation nuclei, condensation of water vapor into liquid water cloud droplets is possible at and above this altitude. An LCL was determined from each radiosonde profile by first calculating an LCL temperature based on surface observations, following published methods (Bolton, 1980). The ascending radiosonde instruments recorded measurements at uneven intervals of roughly 50-300 m at the altitudes and time periods of interest to this study, and the bounding altitude observations containing the LCL temperature were determined for each sonde profile. Only altitudes less than or equal to 1500 m with negative temperature gradients between sequential observations were searched. The temperature gradient was assumed constant between the observations bounding the LCL, and linear interpolation was used to approximate the LCL altitude.

The TWI is a layer often present in the atmosphere in the trade-wind latitudes characterized by a reversal of the usual negative gradient to a positive gradient of warming with increasing altitude. A TWI base was determined from each radiosonde profile following published methods (Cao et al., 2007). The bounding altitudes containing the TWI base were determined by setting the upper bound as the lowest altitude observation with positive temperature gradient dT_p/dz between itself and the next highest observation, greater than 0 °C temperature and 0% RH, with pressure between 70 and 95 kPa. The pressure bounds are for the Atlantic Ocean TWI (Augstein et al., 1974). The lower bounding altitude was set as the observation one below the upper bounding altitude, which necessarily had a negative temperature gradient dT_n/dz below it. Inside the bounding altitude layer, the temperature gradients were then assumed to equal the positive gradient dT_p/dz above the TWI base and the negative gradient dT_n/dz below the TWI base. The intersection of these two lines of constant positive and negative gradient inside the bounding layer was set as the TWI base altitude.

Acknowledgements. This research was supported by the Luquillo Critical Zone Observatory (EAR-1331841) and Grant DEB 1239764 from the U.S. National Science Foundation to the Institute for Tropical Ecosystem Studies, University of Puerto Rico, and to the International Institute of Tropical Forestry (IITF) USDA Forest Service, as part of the Luquillo Long-Term Ecological Research Program. The U.S. Forest Service (Department of Agriculture) Research Unit, the USGS Climate and Land Use Change WEBB Program, and the University of Puerto Rico gave additional support. Samuel Moya, Carlos Estrada, and Carlos Torrens provided field assistance. William A. Gould and Ariel E. Lugo provided comments on an earlier version of the manuscript. Any use of trade, product, or firms names is for descriptive purposes only and does not imply endorsement by the U.S. Government.

© Author(s) 2017. CC-BY 3.0 License.

References

Alvarado-Barrientos, M.S., Holwerda, F., Asbjornsen, H., Dawson, T.E., Bruijnzeel, L.A., 2014. Suppression of transpiration due to cloud immersion in a seasonally dry Mexican weeping pine plantation. Agric. For. Meteorol. 186, 12–25. doi:10.1016/j.agrformet.2013.11.002

Augstein, E., Schmidt, H., Ostapoff, F., 1974. The vertical structure of the atmospheric planetary boundary layer in undisturbed trade winds over the Atlantic Ocean. Bound.-Layer Meteorol. 6, 129–150. doi:10.1007/BF00232480

Bolton, D., 1980. The Computation of Equivalent Potential Temperature. Mon. Weather Rev. 108, 1046–1053. doi:10.1175/1520-0493(1980)108<1046:TCOEPT>2.0.CO;2

Brueck, M., Nuijens, L., Stevens, B., 2014. On the Seasonal and Synoptic Time-Scale Variability of the North Atlantic Trade Wind Region and Its Low-Level Clouds. J. Atmospheric Sci. 72, 1428–1446. doi:10.1175/JAS-D-14-0054.1

Bruijnzeel, L.A., Mulligan, M., Scatena, F.N., 2011. Hydrometeorology of tropical montane cloud forests: emerging patterns. Hydrol. Process. 25, 465–498. doi:10.1002/hyp.7974

Cao, G., Giambelluca, T.W., Stevens, D.E., Schroeder, T.A., 2007. Inversion Variability in the Hawaiian Trade Wind Regime. J. Clim. 20, 1145–1160. doi:10.1175/JCLI4033.1

Carrillo, J., Guerra, J.C., Cuevas, E., Barrancos, J., 2015. Characterization of the Marine Boundary Layer and the Trade-Wind Inversion over the Sub-tropical North Atlantic. Bound.-Layer Meteorol. 158, 311–330. doi:10.1007/s10546-015-0081-1

Cavelier, J., Goldstein, G., 1989. Mist and fog interception in elfin cloud forests in Colombia and Venezuela. J. Trop. Ecol. 5, 309–322. doi:10.1017/S0266467400003709

Comarazamy, D.E., González, J.E., 2011. Regional long-term climate change (1950–2000) in the midtropical Atlantic and its impacts on the hydrological cycle of Puerto Rico. J. Geophys. Res. Atmospheres 116, 1–18. doi:10.1029/2010JD015414

Costa-Surós, M., Calbó, J., González, J.A., Martin-Vide, J., 2013. Behavior of cloud base height from ceilometer measurements. Atmospheric Res. 127, 64–76. doi:10.1016/j.atmosres.2013.02.005

Durre, I., Williams, C.N., Yin, X., Vose, R.S., 2009. Radiosonde-based trends in precipitable water over the Northern Hemisphere: An update. J. Geophys. Res. Atmospheres 114, D05112. doi:10.1029/2008JD010989

Eller, C.B., Lima, A.L., Oliveira, R.S., 2013. Foliar uptake of fog water and transport belowground alleviates drought effects in the cloud forest tree species, Drimys brasiliensis (Winteraceae). New Phytol. 199, 151–162. doi:10.1111/nph.12248

Eugster, W., Burkard, R., Holwerda, F., Scatena, F.N., Bruijnzeel, L.A. (Sampurno), 2006. Characteristics of fog and fogwater fluxes in a Puerto Rican elfin cloud forest. Agric. For. Meteorol. 139, 288–306. doi:10.1016/j.agrformet.2006.07.008

Foster, P., 2001. The potential negative impacts of global climate change on tropical montane cloud forests. Earth-Sci. Rev. 55, 73–106. doi:10.1016/S0012-8252(01)00056-3

Giambelluca, T.W., DeLay, J.K., Nullet, M.A., Scholl, M.A., Gingerich, S.B., 2011. Canopy water balance of windward and leeward Hawaiian cloud forests on Haleakalā, Maui, Hawai'i. Hydrol. Process. 25, 438–447. doi:10.1002/hyp.7738

© Author(s) 2017. CC-BY 3.0 License.

Giannini, A., Kushnir, Y., Cane, M.A., 2000. Interannual Variability of Caribbean Rainfall, ENSO, and the Atlantic Ocean*. J. Clim. 13, 297–311. doi:10.1175/1520-0442(2000)013<0297:IVOCRE>2.0.CO;2

Gotsch, S.G., Nadkarni, N., Darby, A., Glunk, A., Dix, M., Davidson, K., Dawson, T.E., 2015. Life in the treetops: ecophysiological strategies of canopy epiphytes in a tropical montane cloud forest. Ecol. Monogr. 85, 393–412. doi:10.1890/14-1076.1

Gouirand, I., Jury, M.R., Sing, B., 2012. An Analysis of Low- and High-Frequency Summer Climate Variability around the Caribbean Antilles. J. Clim. 25, 3942–3952. doi:10.1175/JCLI-D-11-00269.1

Guo, P., Kuo, Y.-H., Sokolovskiy, S.V., Lenschow, D.H., 2011. Estimating Atmospheric Boundary Layer Depth Using COSMIC Radio Occultation Data. J. Atmospheric Sci. 68, 1703–1713. doi:10.1175/2011JAS3612.1

Holwerda, F., Bruijnzeel, L.A., Scatena, F.N., 2011. Comparison of passive fog gauges for determining fog duration and fog interception by a Puerto Rican elfin cloud forest. Hydrol. Process. 25, 367–373. doi:10.1002/hyp.7641

Hunt, W.H., Winker, D.M., Vaughan, M.A., Powell, K.A., Lucker, P.L., Weimer, C., 2009. CALIPSO Lidar Description and Performance Assessment. J. Atmospheric Ocean. Technol. 26, 1214–1228. doi:10.1175/2009JTECHA1223.1

Jarvis, A., Mulligan, M., 2011. The climate of cloud forests. Hydrol. Process. 25, 327–343. doi:10.1002/hyp.7847

Karmalkar, A.V., Taylor, M.A., Campbell, J., Stephenson, T., New, M., Centella, A., Benzanilla, A., Charlery, J., 2013. A review of observed and projected changes in climate for the islands in the Caribbean. Atmósfera 26, 283–309.

Lawton, R.O., Nair, U.S., Pielke, R.A., Welch, R.M., 2001. Climatic Impact of Tropical Lowland Deforestation on Nearby Montane Cloud Forests. Science 294, 584–587. doi:10.1126/science.1062459

Malkus, J.S., 1955. The effects of a large island upon the trade-wind air stream. Q. J. R. Meteorol. Soc. 81, 538–550. doi:10.1002/qj.49708135003

Martin, P.H., Fahey, T.J., Sherman, R.E., 2011. Vegetation zonation in a neotropical montane forest: environment, disturbance and ecotones. Biotropica 43, 533–543.

Myers, T.A., Norris, J.R., 2013. Observational Evidence That Enhanced Subsidence Reduces Subtropical Marine Boundary Layer Cloudiness. J. Clim. 26, 7507–7524. doi:10.1175/JCLI-D-12-00736.1

Nadolski, V., 1998. Automated Surface Observing System (ASOS) user's guide. Natl. Ocean. Atmospheric Adm. Dep. Def. Fed. Aviat. Adm. U. S. Navy.

Nuijens, L., Serikov, I., Hirsch, L., Lonitz, K., Stevens, B., 2014. The distribution and variability of low-level cloud in the North Atlantic trades. Q. J. R. Meteorol. Soc. 140, 2364–2374.

Odum, H.T., Pigeon, R.F., 1970. A tropical rain forest: a study of irradiation and ecology at El Verde, Puerto Rico. US Atomic Energy Commission, Division of Technical Information, Washington, DC (EUA).

Oliveira, R.S., Eller, C.B., Bittencourt, P.R.L., Mulligan, M., 2014. The hydroclimatic and ecophysiological basis of cloud forest distributions under current and projected climates. Ann. Bot. 113, 909–920. doi:10.1093/aob/mcu060

Perez, T.M., Stroud, J.T., Feeley, K.J., 2016. Thermal trouble in the tropics. Science 351, 1392–1393. doi:10.1126/science.aaf3343

© Author(s) 2017. CC-BY 3.0 License.

Raga, G.B., Baumgardner, D., Mayol-Bracero, O.L., 2016. History of Aerosol-Cloud Interactions Derived from Observations in Mountaintop Clouds in Puerto Rico. Aerosol Air Qual. Res. 16, 674–688.

Rastogi, B., Williams, A.P., Fischer, D.T., Iacobellis, S., McEachern, K., Carvalho, L., Jones, C., Baguskas, S.A., Still, C.J., 2016. Spatial and temporal patterns of cloud cover and fog inundation in coastal California: Ecological implications. Earth Interact. doi:10.1175/EI-D-15-0033.1

Ray, D.K., Welch, R.M., Lawton, R.O., Nair, U.S., 2006. Dry season clouds and rainfall in northern Central America: Implications for the Mesoamerican Biological Corridor. Glob. Planet. Change, Land-use/land-cover change and its impact on climate 54, 150–162. doi:10.1016/j.gloplacha.2005.09.004

Scholl, M.A., Murphy, S.F., 2014. Precipitation isotopes link regional climate patterns to water supply in a tropical mountain forest, eastern Puerto Rico. Water Resour. Res. 50, 4305–4322. doi:10.1002/2013WR014413

Schulz, H.M., Thies, B., Chang, S.-C., Bendix, J., 2016. Detection of ground fog in mountainous areas from MODIS (Collection 051) daytime data using a statistical approach. Atmospheric Meas. Tech. 9.

Stevens, B., 2005. Atmospheric Moist Convection. Annu. Rev. Earth Planet. Sci. 33, 605–643. doi:10.1146/annurev.earth.33.092203.122658

Still, C.J., Foster, P.N., Schneider, S.H., 1999. Simulating the effects of climate change on tropical montane cloud forests. Nature 398, 608–610. doi:10.1038/19293

Taylor, M.A., Alfaro, E.J., 2005. Central America and the Caribbean, Climate of, in: Oliver, J.E. (Ed.), Encyclopedia of World Climatology, Encyclopedia of Earth Sciences Series. Springer Netherlands, pp. 183–189. doi:10.1007/1-4020-3266-8_37

Taylor, M.A., Whyte, F.S., Stephenson, T.S., Campbell, J.D., 2013. Why dry? Investigating the future evolution of the Caribbean Low Level Jet to explain projected Caribbean drying. Int. J. Climatol. 33, 784–792. doi:10.1002/joc.3461

Van Beusekom, A.E., González, G., Rivera, M.M., 2015. Short-Term Precipitation and Temperature Trends along an Elevation Gradient in Northeastern Puerto Rico. Earth Interact. 19, 1–33.

van der Molen, M.K., Dolman, A.J., Waterloo, M.J., Bruijnzeel, L.A., 2006. Climate is affected more by maritime than by continental land use change: A multiple scale analysis. Glob. Planet. Change, Land-use/land-cover change and its impact on climate 54, 128–149. doi:10.1016/j.gloplacha.2006.05.005

Weaver, P.L., 1995. The Colorado and Dwarf Forests of Puerto Rico's Luquillo Mountains, in: Lugo, A.E., Lowe, C. (Eds.), Tropical Forests: Management and Ecology, Ecological Studies. Springer New York, pp. 109–141. doi:10.1007/978-1-4612-2498-3_5

Weaver, P.L., Gould, W.A., 2013. Forest vegetation along environmental gradients in northeastern Puerto Rico. Ecol. Bull. 54, 43–65.

Wohl, E., Barros, A., Brunsell, N., Chappell, N.A., Coe, M., Giambelluca, T., Goldsmith, S., Harmon, R., Hendrickx, J.M.H., Juvik, J., McDonnell, J., Ogden, F., 2012. The hydrology of the humid tropics. Nat. Clim. Change 2, 655–662. doi:10.1038/nclimate1556

Atmos. Chem. Phys. Discuss., doi:10.5194/acp-2016-1166, 2017
Manuscript under review for journal Atmos. Chem. Phys.
Published: 7 February 2017
© Author(s) 2017. CC-BY 3.0 License.

Zhang, C., Wang, Y., Lauer, A., Hamilton, K., Xie, F., 2012. Cloud base and top heights in the Hawaiian region determined with satellite and ground-based measurements. Geophys. Res. Lett. 39, L15706. doi:10.1029/2012GL052355

Atmos. Chem. Phys. Discuss., doi:10.5194/acp-2016-1166, 2017
Manuscript under review for journal Atmos. Chem. Phys.
Published: 7 February 2017
© Author(s) 2017. CC-BY 3.0 License.

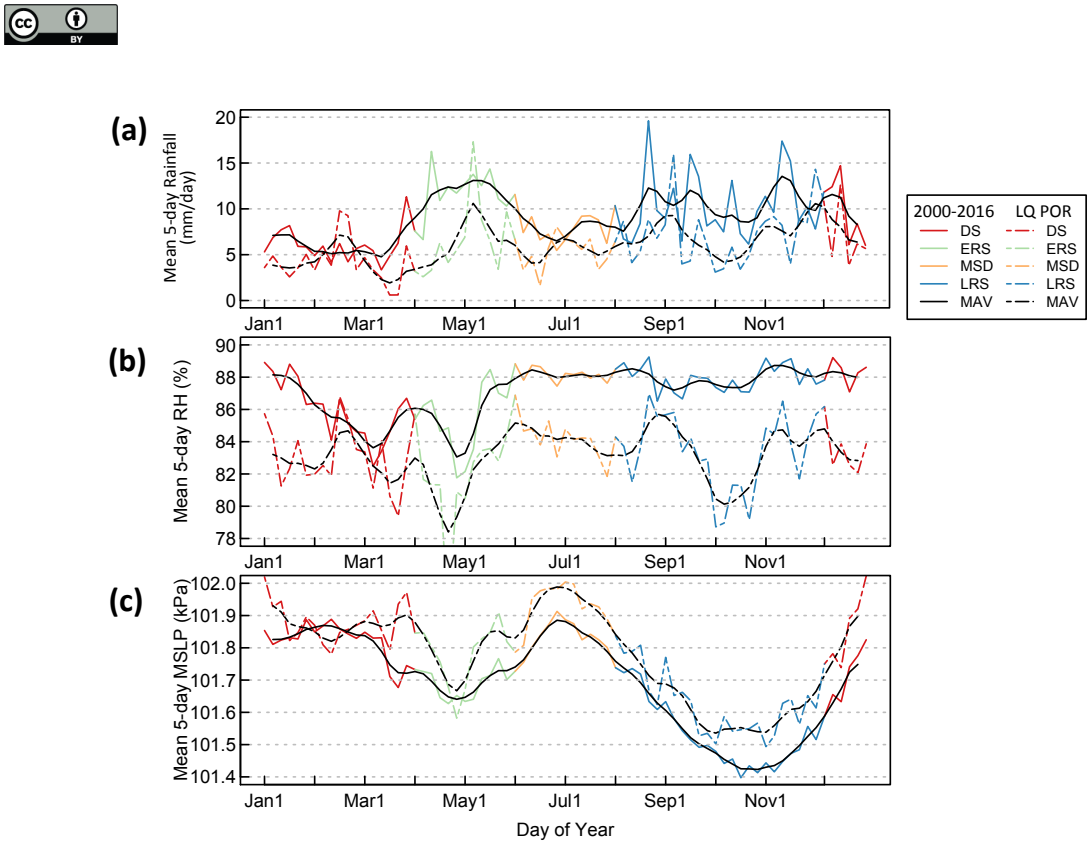

Figure 1: Day of year mean values for: a) precipitation at 361 m; b) relative humidity (RH) at 361 m; and c) mean sea level pressure (MSLP) at 100 m in the Luquillo study area. The colors show the 5-day means during dry season (DS), early rain season (ERS), mid-summer drought (MSD), and late rain season (LRS). The black line is the 15-day moving average (MAV), with the 2000-2016 period as solid lines and the Luquillo period of record (LQ POR) of May 2013 through August 2016 as dashed lines.

Atmos. Chem. Phys. Discuss., doi:10.5194/acp-2016-1166, 2017
Manuscript under review for journal Atmos. Chem. Phys.
Published: 7 February 2017
© Author(s) 2017. CC-BY 3.0 License.

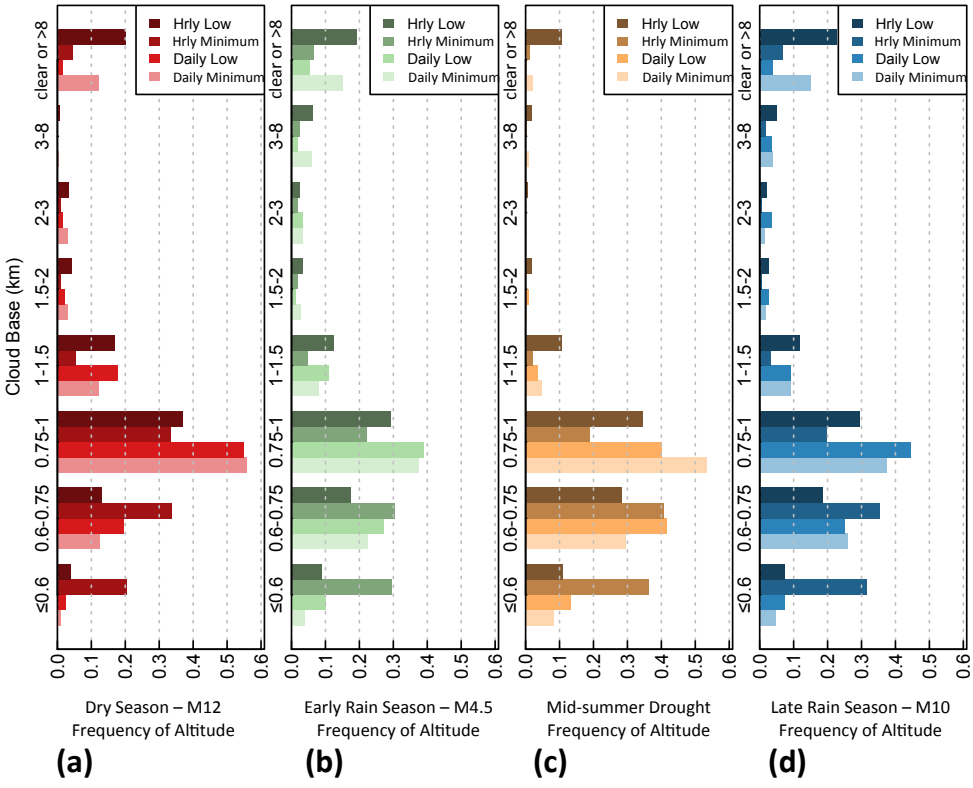

Figure 2: Frequency of low cloud base by season excluding non-representative months in each year: a) dry season without month December (M12); b) early rain season without April 1-15 (M4.5); c) mid-summer drought; d) late rain season without October (M10). The metrics are hourly low cloud base (first quartile (Q_1) of each hour of 30-second cloud base altitudes), hourly minimum value, daily low value (first tertile (T_1) of the hourly low set), and daily minimum value (seventh octile (O_7) of the hourly minimum set).

Atmos. Chem. Phys. Discuss., doi:10.5194/acp-2016-1166, 2017
Manuscript under review for journal Atmos. Chem. Phys.
Published: 7 February 2017
© Author(s) 2017. CC-BY 3.0 License.

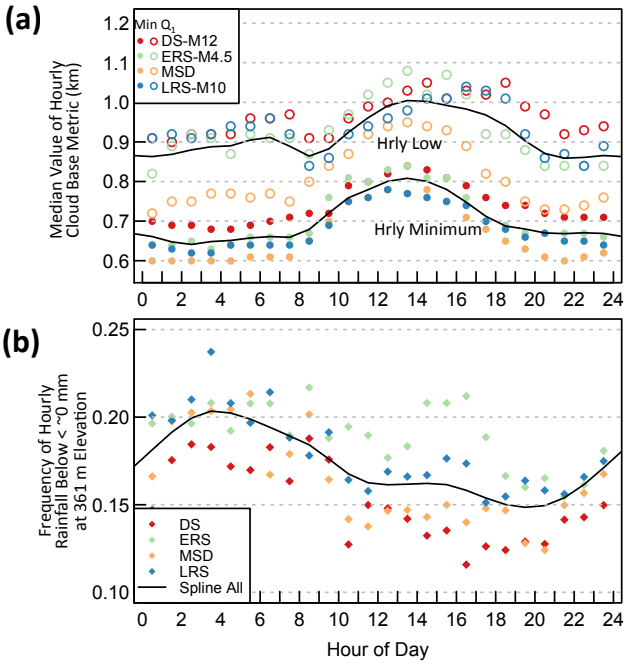

Figure 3: Summaries of cloud base altitude by hour of day for Luquillo period of record (LQ POR) for dry season without month December (DS – M12), early rain season without April 1-15 (ERS – M4.5), mid-summer drought (MSD), and late rain season without October (LRS – M10): a) median altitude of hourly low cloud bases and median altitude of hourly minimum cloud bases; b) frequency of no measureable rainfall in each hour of the day for 2000-2016 for Bisley station at 361 m elevation. Colored symbols are seasonal values and black lines are the cubic smoothing splines of all data in the LQ POR.

Atmos. Chem. Phys. Discuss., doi:10.5194/acp-2016-1166, 2017
Manuscript under review for journal Atmos. Chem. Phys.
Published: 7 February 2017
© Author(s) 2017. CC-BY 3.0 License.

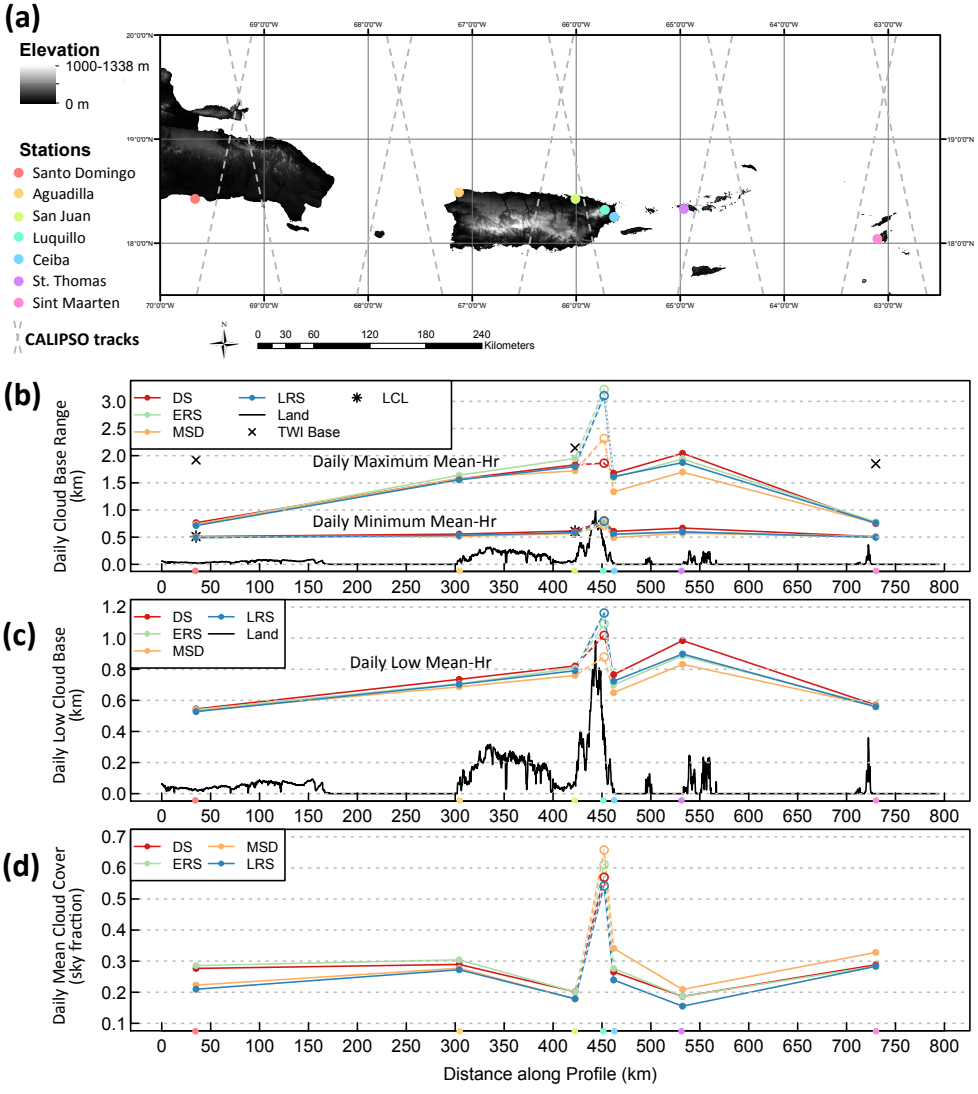

Figure 4. Daily 'usual' mean clouds averaged over the dry season (DS), early rain season (ERS), mid-summer drought (MSD), and late rain season (LRS) for the period of record (POR) across the region: a) locations of airport ASOS stations, Luquillo station, and CALIPSO satellite tracks, along with topography; b) daily minimum and maximum cloud bases (of hourly means), land surface elevation along profile, and calculated trade wind inversion (TWI) base and lifting condensation level (LCL) where available; c) daily low cloud base (first quartile (Q_1) of hourly means) and land surface elevation along profile; d) daily mean cloud cover as fraction of sky. The land surface profile trends due east and west (shifting north and south to be near the stations). Station locations are marked with circles on the x-axis in the same colors as plot a. Dashed colored lines between San Juan and Ceiba are used to indicate that the Luquillo station measurements are only based on the available Luquillo POR May 2013-August 2016 excluding non-representative months the entire 2000-2016. 'Usual' defined as hours with cloud cover at least 50% of mean-POR cloud cover for station.

Atmos. Chem. Phys. Discuss., doi:10.5194/acp-2016-1166, 2017
Manuscript under review for journal Atmos. Chem. Phys.
Published: 7 February 2017
© Author(s) 2017. CC-BY 3.0 License.

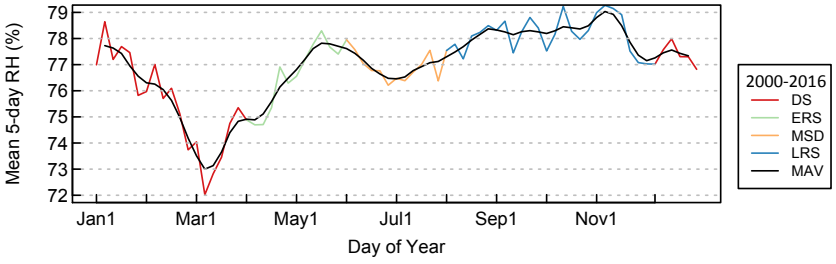

Figure 5. Day of year mean values for relative humidity (RH) averaged over all airport ASOS stations (does not include Luquillo). The colors show the 5-day means during dry season (DS), early rain season (ERS), mid-summer drought (MSD), and late rain season (LRS). The black line is the 15-day moving average (MAV) for the 2000-2016.

Atmos. Chem. Phys. Discuss., doi:10.5194/acp-2016-1166, 2017
Manuscript under review for journal Atmos. Chem. Phys.
Published: 7 February 2017
© Author(s) 2017. CC-BY 3.0 License.

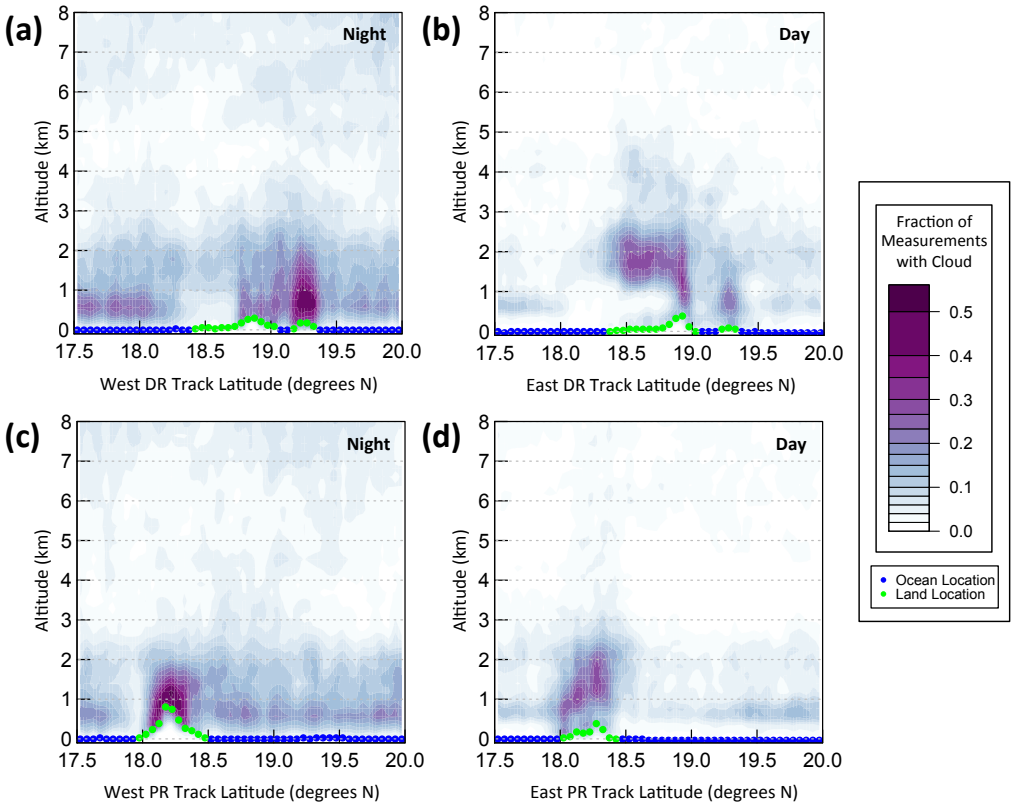

Figure 6. CALIPSO satellite data fraction of measurements with cloud recorded in cell, for years 2006-2016 with cell as 0.05° latitude along track and 30 m altitude for: a) West Dominican Republic (DR) track (night orbit); b) East DR track (day orbit); c) West Puerto Rico (PR) track (night orbit); and d) East PR track (day orbit). Since track measurement location varies slightly, surface point (land or ocean) is plotted as the mean location. Cell fractions are spline-smoothed into a surface.

Atmos. Chem. Phys. Discuss., doi:10.5194/acp-2016-1166, 2017
Manuscript under review for journal Atmos. Chem. Phys.
Published: 7 February 2017
© Author(s) 2017. CC-BY 3.0 License.

Atmospheric Chemistry and Physics Discussions

Station	Lat (° N)	Long (° W)	Elev (m)	Land Cover	Variables‡	Period Used	Data Missing	Data Reference
Sabana LQ*†	18.32	65.73	100	Forest	RF, RH, MSLP, T, WD, WS	5/2013 – 8/2016	5%	https://www.sciencebase.gov
Bisley LQ*	18.30	65.75	361	Forest	RF, RH, T, WD, WS	1/2000 – 8/2016	3%	https://www.sciencebase.gov
Icacos LQ*	18.28	65.79	645	TMCF	RF	1/2000 – 1/2016	7%	50075000 http://waterdata.usgs.gov/nwis
Santo Domingo†	18.43	69.67	18	Airport	RH, T, WD, WS, S	1/2000 – 8/2016	28%	MDSD http://mesonet.agron.iastate.edu
Aquadilla†	18.49	67.13	72	Airport	RH, T, WD, WS	1/2000 – 8/2016	35%	TJBQ http://mesonet.agron.iastate.edu
San Juan†	18.43	66.01	3	Airport	RF, RH, MSLP, T, WD, WS, S	1/2000 – 8/2016	1%	TJSJ http://mesonet.agron.iastate.edu
Ceiba†	18.26	65.64	12	Airport	RF, RH, MSLP, T, WD, WS	1/2000 – 8/2016	37%	TJNR http://mesonet.agron.iastate.edu
St. Thomas†	18.34	64.97	7	Airport	RF, RH, MSLP, T, WD, WS	1/2000 – 8/2016	6%	TIST http://mesonet.agron.iastate.edu
Sint Maarten†	18.04	63.11	4	Airport	RH, T, WD, WS, S	1/2000 – 8/2016	7%	TISM http://mesonet.agron.iastate.edu
CALIPSO tracks†	17.5-20	62.5-70	vary	Various	Cloud vertical profiles	6/2006 – 8/2016	0.05%	http://www-calipso.larc.nasa.gov

* Near Luquillo (LQ)

† Cloud data collected at these stations

‡ Key to abbreviations: RF = rainfall, RH = relative humidity, MSLP = mean sea level pressure, T = temperature, WD = wind direction, WS = wind speed, S = radiosonde

Table 1. Data Record Information.

Atmos. Chem. Phys. Discuss., doi:10.5194/acp-2016-1166, 2017
Manuscript under review for journal Atmos. Chem. Phys.
Published: 7 February 2017
© Author(s) 2017. CC-BY 3.0 License.

Atmospheric Chemistry and Physics Discussions

Variable	Cloud Base Altitude				Rainfall	
	Daily Low (Daily T_1 of Q_1 of each hour)		Daily Minimum (Daily O_7 of min of each hour)			
	5-day ρ	Month ρ	5-day ρ	Month ρ	5-day ρ	Month ρ
RH	**-0.34**	**-0.31**	**-0.36**	**-0.28**	**0.13**	*0.05*
MSLP	**-0.45**	**-0.58**	**-0.52**	**-0.54**	**-0.30**	**-0.46**
Cloud Cover	**-0.69**	**-0.76**	**-0.72**	**-0.75**	**0.26**	*0.21*

Significant relationships indicated by typeface: **p-value < 0.1**, p-value < 0.05, **p-value < 0.01**

Insignificant relationships *italicized*.

Table 2. Correlations Coefficients ρ of Relative Humidity (RH), Mean Sea Level Pressure (MSLP), and Cloud Cover with Cloud Base Altitude Metrics and Rainfall near the Luquillo Ceilometer.

Atmos. Chem. Phys. Discuss., doi:10.5194/acp-2016-1166, 2017
Manuscript under review for journal Atmos. Chem. Phys.
Published: 7 February 2017
© Author(s) 2017. CC-BY 3.0 License.

Atmospheric Chemistry and Physics Discussions

Variable	Station	Cloud Base Altitude						Rainfall	
		Daily Low Mean-Hour (Q_1 of usual hrly means)		Daily Minimum Mean-Hour (min of usual hrly means)		Daily Maximum Mean-Hour (max of usual hrly means)			
		5-day ρ	Month ρ	5-day ρ	Month ρ	5-day ρ	Month ρ	5-day ρ	Month ρ
RH	ASOS all*	**-0.35**	**-0.30**	-0.36	*-0.26*	*-0.06*	*-0.17*	NA	NA
	ASOS near†	**-0.36**	**-0.29**	**-0.47**	*-0.33*	*-0.01*	*-0.08*	**0.22**	**0.17**
	Luquillo‡	**-0.22**	*-0.19*	**-0.37**	-0.36	*0.04*	*-0.01*	**0.13**	*0.05*
MSLP	ASOS all*	NA	NA	NA	NA	NA	NA	NA	NA
	ASOS near†	*0.04*	*0.01*	**0.17**	**0.14**	**-0.10**	*-0.08*	**-0.27**	**-0.42**
	Luquillo‡	**-0.40**	**-0.64**	-0.18	**-0.30**	**-0.45**	**-0.57**	**-0.30**	**-0.46**
Cloud	ASOS all*	-0.21	*-0.18*	**-0.18**	*-0.08*	*0.02*	*0.01*	NA	NA
Cover	ASOS near†	**-0.30**	**-0.42**	**-0.27**	**-0.28**	**-0.03**	*-0.14*	*-0.01*	*-0.10*
	Luquillo‡	**-0.46**	**-0.76**	**-0.47**	**-0.82**	*-0.06*	-0.37	**0.26**	*0.21*

Significant relationships indicated by typeface: **p-value < 0.1**, p-value < 0.05, **p-value <0.01**

Insignificant relationships *italicized*.

* Mean of ρ from all six airport ASOS stations 2000-2015

† Mean of ρ from three airport ASOS stations nearest to Luquillo 2000-2015: San Juan, Ceiba, St. Thomas

‡ ρ from station 5/2013 – 12/2015

'Usual' defined as hours with cloud cover at least 50% of mean-POR cloud cover for station.

Table 3. Correlation Coefficients ρ of Relative Humidity (RH), Mean Sea Level Pressure (MSLP), and Cloud Cover with Cloud Base Altitude Metrics and rainfall Region-Wide.